JCI The Journal of Clinical Investigation

Plasma fibronectin supports hemostasis and regulates thrombosis

Yiming Wang, … , John Freedman, Heyu Ni

J Clin Invest. 2014;124(10):4281-4293. https://doi.org/10.1172/JCI74630.

Research Article Hematology

Plasma fibronectin (pFn) has long been suspected to be involved in hemostasis; however, direct evidence has been lacking. Here, we demonstrated that pFn is vital to control bleeding in fibrinogen-deficient mice and in WT mice given anticoagulants. At the site of vessel injury, pFn was rapidly deposited and initiated hemostasis, even before platelet accumulation, which is considered the first wave of hemostasis. This pFn deposition was independent of fibrinogen, von Willebrand factor, β3 integrin, and platelets. Confocal and scanning electron microscopy revealed pFn integration into fibrin, which increased fibrin fiber diameter and enhanced the mechanical strength of clots, as determined by thromboelastography. Interestingly, pFn promoted platelet aggregation when linked with fibrin but inhibited this process when fibrin was absent. Therefore, pFn may gradually switch from supporting hemostasis to inhibiting thrombosis and vessel occlusion following the fibrin gradient that decreases farther from the injured endothelium. Our data indicate that pFn is a supportive factor in hemostasis, which is vital under both genetic and therapeutic conditions of coagulation deficiency. By interacting with fibrin and platelet β3 integrin, pFn plays a self-limiting regulatory role in thrombosis, suggesting pFn transfusion may be a potential therapy for bleeding disorders, particularly in association with anticoagulant therapy.

Plasma fibronectin supports hemostasis and regulates thrombosis

Yiming Wang,[1,2,3] Adili Reheman,[2] Christopher M. Spring,[2] Jalil Kalantari,[2,4] Alexandra H. Marshall,[2] Alisa S. Wolberg,[5] Peter L. Gross,[6] Jeffrey I. Weitz,[6] Margaret L. Rand,[1,7] Deane F. Mosher,[8] John Freedman,[1,2,9] and Heyu Ni[1,2,3,4,9]

[1]Department of Laboratory Medicine and Pathobiology, University of Toronto, Toronto, Ontario, Canada. [2]Toronto Platelet Immunobiology Group and Department of Laboratory Medicine, Keenan Research Centre for Biomedical Science of St. Michael's Hospital, Toronto, Ontario, Canada. [3]Canadian Blood Services, Toronto, Ontario, Canada. [4]Department of Physiology, University of Toronto, Toronto, Ontario, Canada. [5]Department of Pathology and Laboratory Medicine, University of North Carolina at Chapel Hill, Chapel Hill, North Carolina, USA. [6]McMaster University and Thrombosis and Atherosclerosis Research Institute, Hamilton, Ontario, Canada. [7]Division of Haematology/Oncology, The Hospital for Sick Children, Toronto, Ontario, Canada. [8]Departments of Biomolecular Chemistry and Medicine, University of Wisconsin, Madison, Wisconsin, USA. [9]Department of Medicine, University of Toronto, Toronto, Ontario, Canada.

Plasma fibronectin (pFn) has long been suspected to be involved in hemostasis; however, direct evidence has been lacking. Here, we demonstrated that pFn is vital to control bleeding in fibrinogen-deficient mice and in WT mice given anticoagulants. At the site of vessel injury, pFn was rapidly deposited and initiated hemostasis, even before platelet accumulation, which is considered the first wave of hemostasis. This pFn deposition was independent of fibrinogen, von Willebrand factor, β3 integrin, and platelets. Confocal and scanning electron microscopy revealed pFn integration into fibrin, which increased fibrin fiber diameter and enhanced the mechanical strength of clots, as determined by thromboelastography. Interestingly, pFn promoted platelet aggregation when linked with fibrin but inhibited this process when fibrin was absent. Therefore, pFn may gradually switch from supporting hemostasis to inhibiting thrombosis and vessel occlusion following the fibrin gradient that decreases farther from the injured endothelium. Our data indicate that pFn is a supportive factor in hemostasis, which is vital under both genetic and therapeutic conditions of coagulation deficiency. By interacting with fibrin and platelet β3 integrin, pFn plays a self-limiting regulatory role in thrombosis, suggesting pFn transfusion may be a potential therapy for bleeding disorders, particularly in association with anticoagulant therapy.

Introduction

Platelet accumulation and coagulation system activation are two key mechanisms required to stop bleeding (1–3). At the site of vascular injury, subendothelial matrix exposure initiates platelet adhesion, activation, and aggregation, which constitute the first wave of hemostasis (or primary hemostasis). Exposure of tissue factor and procoagulant cell membranes activates the coagulation cascade, a series of enzymatic reactions leading to the formation of a fibrin clot (i.e., the second wave of hemostasis or secondary hemostasis). However, if platelets and coagulation are inappropriately activated, thrombosis and vessel occlusion may occur, which can lead to life-threatening conditions, including myocardial infarction and stroke, the major causes of mortality and morbidity worldwide (4). A better understanding of the mechanisms underlying thrombosis is crucial for treatment and prevention of thrombotic and hemorrhagic disorders.

Fibronectin (Fn), a dimer of 250-kDa subunits, is a key component of the extracellular matrix and is required for embryonic development (5). Fn exists as plasma Fn (pFn) and cellular Fn. Unlike cellular Fn, which is produced by various cell types and deposits locally, pFn is synthesized in the liver and secreted into the blood, in which it circulates at a relatively high concentration (230–650 μg/ml) (6, 7). Both subunits of the Fn dimer contain N terminus fibrin and collagen-binding sites as well as a C terminus arginine-glycine-aspartic acid (RGD) motif (i.e., the integrin-binding site). The N terminus collagen-binding site may play a role in mediating the incorporation of pFn into the vessel wall (8, 9). Collagen, a major subendothelial matrix protein, can be easily exposed to blood components after the denudation of endothelial cells following injury. However, the efficiency of this pFn-collagen interaction under flow conditions and whether this process contributes to hemostasis in vivo have not been elucidated. The N terminus of pFn can also cross-link to the C terminus of the fibrin α chain by factor XIIIa (FXIIIa), thus enabling pFn incorporation into fibrin clots (10). Notably, Fn, fibrinogen (Fg), components of the coagulation cascade, and the type I Fn module (present 12 times in Fn and as single modules in several cascade components) arose together in evolution and are all vertebrate inventions (11–13). Despite these intriguing observations, there is no evidence supporting a significant contribution of pFn to blood coagulation. The C terminus RGD motif on pFn is also relevant to hemostasis; through binding to integrins on endothelial cells, fibroblasts, and adherent platelets, a pFn matrix can assemble on these cell surfaces (14–16), which may contribute to platelet accu-

Note regarding evaluation of this manuscript: Manuscripts authored by scientists associated with Duke University, The University of North Carolina at Chapel Hill, Duke-NUS, and the Sanford-Burnham Medical Research Institute are handled not by members of the editorial board but rather by the science editors, who consult with selected external editors and reviewers.

Conflict of interest: The authors have declared that no conflict of interest exists.

Submitted: March 7, 2014; **Accepted:** July 24, 2014.

Reference information: *J Clin Invest*. 2014;124(10):4281–4293. doi:10.1172/JCI74630.

Table 1. High mortality rate in mice with combined deficiencies of both Fg and pFn

	Total no. of mice	No. of dead mice	Mortality (%)
pFn$^{+/+}$ *FG*$^{-/-}$	55	3	5.5%
FG$^{-/-}$ *pFn*$^{-/-}$	53	12	22.6%[A]
pFn$^{+/+}$ *Vwf*$^{-/-}$	57	1	1.8%
Vwf$^{-/-}$ *pFn*$^{-/-}$	51	0	0%
pFn$^{+/+}$ *FG*$^{-/-}$ *Vwf*$^{-/-}$	66	6	9.1%
TKO	78	18	23.1%[A]

Mortality rate was calculated 1 month after polyinonic-polycytidylic acid injection. [A]$P < 0.05$.

mulation and hemostatic plug formation. Moreover, as we demonstrated previously, circulating pFn can be taken up by platelets via β3 integrin (17), particularly in the absence of Fg competition (17, 18). Although the role of this internalized pFn has not been well studied, it is conceivable that increased platelet pFn content may be a compensatory mechanism to support hemostasis in individuals with afibrinogenemia. The abundance of pFn in the plasma and within platelets, as well as its interaction with components of the subendothelial matrix and coagulation cascade, has led to a long-held suspicion that pFn may play a role in hemostasis (3, 18–20), but there has been no direct in vivo evidence.

Germ line Fn deficiency is embrionic lethal in mice (5). Our earlier study with pFn conditional knockout mice using intravital microscopy revealed that pFn promotes thrombus growth and stability in injured arterioles (19, 21). We also reported that platelet aggregation and thrombus formation persist in mice lacking Fg, von Willebrand factor (VWF), or both (18, 22); Fg and VWF have been considered to be the two key molecules mediating platelet adhesion and aggregation. In the absence of Fg or both Fg and VWF, platelet pFn content is markedly increased in mice and human patients (18, 23, 24). It was therefore speculated that pFn may be the factor that mediates this Fg/VWF-independent thrombus formation. Paradoxically, we observed that depletion of pFn in mice doubly deficient in Fg and VWF (*FG*$^{-/-}$ *Vwf*$^{-/-}$) enhances, rather than abolishes, platelet aggregation and thrombus formation (25). These findings led us to hypothesize that pFn has context-specific functions (i.e., a functional switch based on the presence of Fg and/or VWF) in the hemostatic system such that pFn can both support hemostatic plug formation and inhibit thrombus buildup. However, the mechanisms that mediate the switch of pFn functions are unknown.

To investigate the role of pFn in hemostasis and the mechanism that controls the context-specific functions of pFn (i.e., whether Fg or VWF dictated the pFn functional switch), using a conditional transgenic mouse (*Fn*$^{fl/fl}$ *Mx-Cre* mice, referred to herein as *pFn*$^{-/-}$ mice) (21), we established Fg and pFn double-deficient (*FG*$^{-/-}$ *pFn*$^{-/-}$) and VWF and pFn double-deficient (*Vwf*$^{-/-}$ *pFn*$^{-/-}$) mouse strains. We found that pFn is a vital survival factor for hemostasis in Fg deficiency and supports hemostasis in VWF deficiency. We showed that pFn deposition precedes the classical first wave of hemostasis (i.e., platelet accumulation) in both WT and these deficient mice. pFn integrates with fibrin, controls the diameter of fibrin fibers, increases the mechanical strength of the clot, and is actively involved in thrombosis. Through switching its function in platelet aggregation, based on the presence or absence of fibrin (not VWF), pFn provides a self-limiting mechanism that prevents excessive platelet accumulation and vessel occlusion. These findings provide a solution for the controversy surrounding the function of pFn in hemostasis and establish pFn as a unique regulatory factor in thrombosis.

Results

pFn is a vital hemostatic factor in Fg deficiency. Conditional knockout of pFn in mice results in depletion of plasma pFn (>98%) in *Cre*$^{+}$ mice but not in *Cre*$^{-}$ controls (21, 25). Although a previous study with pFn single-deficient mice did not report significantly impaired hemostasis with a tail bleeding assay (21), we encountered markedly increased mortality due to severe bleeding in *FG*$^{-/-}$ *Vwf*$^{-/-}$ *pFn*$^{-/-}$ (TKO) mice (18 of 78, 23.1%) compared with that in their *pFn*$^{+/+}$ *FG*$^{-/-}$ *Vwf*$^{-/-}$ littermates (6 of 66, 9.1%, $P < 0.05$) (Figure 1A and Table 1). Severe bleeding in pFn-depleted mice was observed several days after the pFn levels decreased, and most of the deaths occurred within 1 to 2 weeks of pFn depletion. Autopsy revealed severe subcutaneous and/or abdominal bleeding (Figure 1A). The tail bleeding time in TKO mice mice that survived the first month following pFn depletion was significantly longer than that in their *pFn*$^{+/+}$ *FG*$^{-/-}$ *Vwf*$^{-/-}$ littermates (Figure 1B). In half of the TKO mice (4 of 8), the bleeding did not stop spontaneously within the observed time, whereas most of the *pFn*$^{+/+}$ *FG*$^{-/-}$ *Vwf*$^{-/-}$ mice (10 of 11) achieved hemostasis spontaneously.

To determine whether the increased mortality after pFn depletion was due to an associated deficiency in Fg or VWF, we established 2 new strains of doubly deficient mice, *FG*$^{-/-}$ *pFn*$^{-/-}$ and *Vwf*$^{-/-}$ *pFn*$^{-/-}$ mice. There was no significant difference in blood cell counts or in the expression of major platelet surface adhesion molecules between *pFn*$^{-/-}$ and *pFn*$^{+/+}$ *Cre*$^{-}$ littermates (Supplemental Table 1 and Supplemental Figure 1; supplemental material available online with this article; doi:10.1172/JCI74630DS1). The mortality rate following pFn depletion was significantly higher in *FG*$^{-/-}$ *pFn*$^{-/-}$ mice than in *pFn*$^{+/+}$ *FG*$^{-/-}$ littermates (22.6% and 5.5%, respectively; $P < 0.05$) (Table 1). Similar to the TKO mice, death was due to severe subcutaneous and/or abdominal bleeding. We found that tail bleeding time was also markedly prolonged in *FG*$^{-/-}$ *pFn*$^{-/-}$ mice compared with that in *pFn*$^{+/+}$ *FG*$^{-/-}$ littermates (Figure 1C), and half of the *FG*$^{-/-}$ *pFn*$^{-/-}$ mice did not stop bleeding spontaneously (7 of 14), while only 2 *FG*$^{-/-}$ mice bled beyond the observed time (2 of 11). Although there was no significant difference in the mortality rates of *Vwf*$^{-/-}$ *pFn*$^{-/-}$ and *pFn*$^{+/+}$ *Vwf*$^{-/-}$ littermates (Table 1), the tail bleeding time in *Vwf*$^{-/-}$ *pFn*$^{-/-}$ mice was significantly longer (Supplemental Figure 2). These results suggest that Fg, but not VWF, deficiency, was associated with the increased mortality after pFn depletion and that pFn is an essential hemostatic factor in Fg deficiency, and pFn contributes to hemostasis in VWF deficiency.

We next examined whether transfusion of purified pFn could ameliorate the severe bleeding phenotype in *FG*$^{-/-}$ *pFn*$^{-/-}$ mice. As a considerable amount of Fg contamination was found in commercial pFn and pFn purified from WT mice (Supplemental Figure 3B), pFn used in this study was purified from blood collected

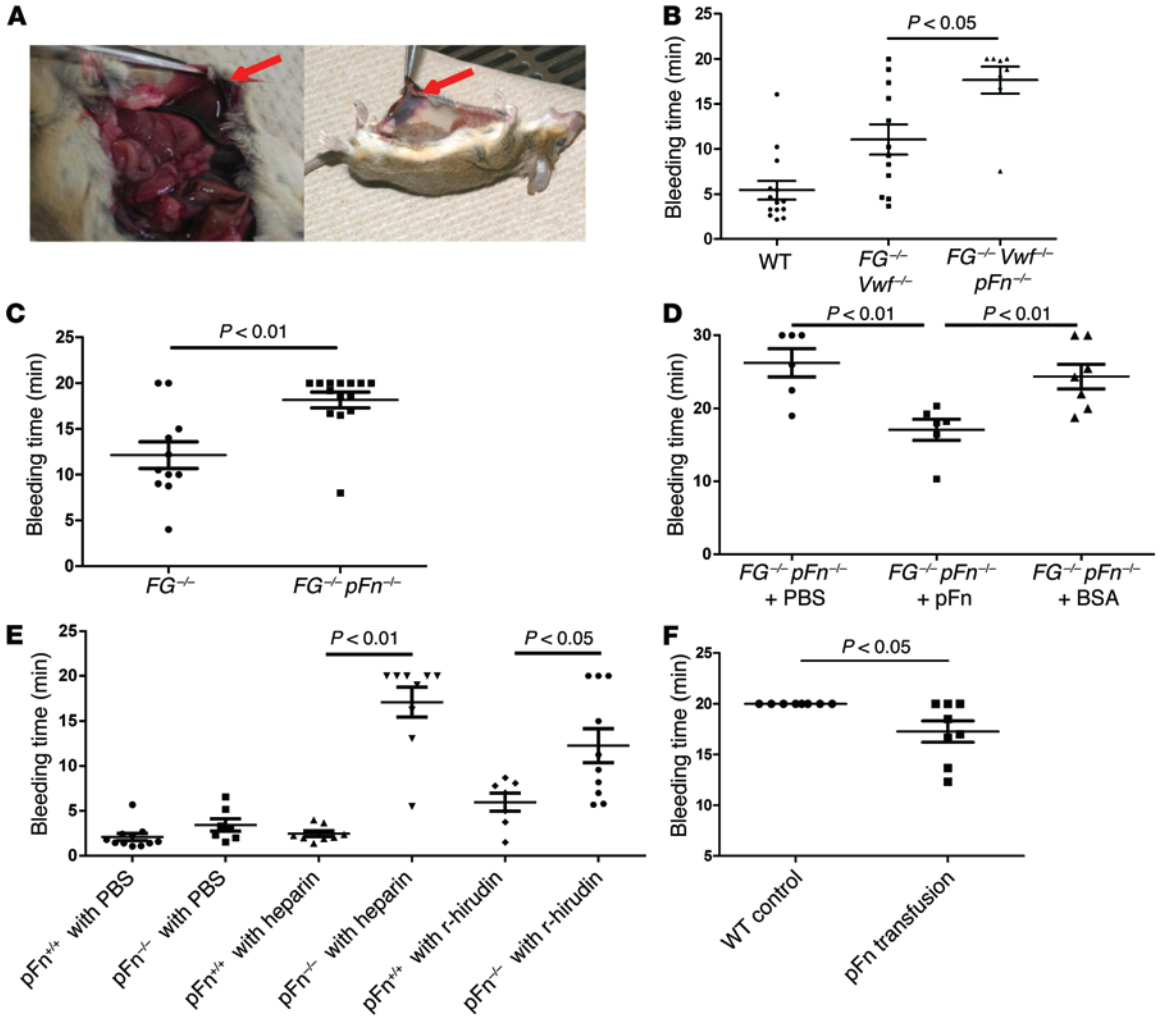

Figure 1. pFn is a key hemostatic factor in deficiencies of Fg and blood coagulation. (**A**) Representative images of abdominal and subcutaneous bleeding in TKO mice. Red arrows show the bleeding site. (**B**) Tail bleeding time in WT, *FG*$^{-/-}$ *Vwf*$^{-/-}$, and TKO mice. (**C**) Tail bleeding time in *FG*$^{-/-}$ and *FG*$^{-/-}$ *pFn*$^{-/-}$ mice. (**D**) Tail bleeding time in *FG*$^{-/-}$ *pFn*$^{-/-}$ mice transfused with 200 μl PBS, 1.5 mg/ml purified pFn, or BSA. (**E**) Tail bleeding time in *pFn*$^{-/-}$ mice and their WT (*pFn*$^{+/+}$) littermates treated with i.p. injection of PBS, 20 U heparin, or 0.5 mg/kg recombinant hirudin (r-hirudin). Tail bleeding assay was performed 30 minutes after the injection. (**F**) Tail bleeding time in WT mice given high-dose heparin (200 U) and then transfused with PBS or pFn. For all tail bleeding assays, 2 mm of the tip of the tail was severed. Bleeding time assay was terminated at 20 or 30 minutes, as indicated, and mice that bled beyond this end point were counted as 20 or 30 minutes, respectively. Data are presented as mean ± SEM. Individual symbols represent individual mice.

from *FG*$^{-/-}$ mice (Supplemental Figure 3, A and B). Compared with transfusion of 200 μl PBS or BSA solution, transfusion of the same volume of pFn solution (1.5 mg/ml, 200 μl) significantly shortened the tail bleeding time in *FG*$^{-/-}$ *pFn*$^{-/-}$ mice (Figure 1D). All of the mice transfused with pFn achieved hemostasis spontaneously within 20 minutes, whereas, even after 30 minutes, bleeding failed to stop in 3 of 6 mice transfused with PBS and in 2 of 7 mice transfused with BSA. This is strong evidence that pFn supports hemostasis in vivo and is a key survival factor in Fg deficiency.

pFn is important for hemostasis following treatment with anticoagulants. Anticoagulants, such as heparin and hirudin, have been widely used for prevention and treatment of thrombosis by inhibiting thrombin function and conversion of Fg to fibrin. In patients on anticoagulant therapy, major bleeding complications occur and are associated with increased mortality. Here, we found that after heparin treatment (20 U, i.p.) the tail bleeding time in *pFn*$^{-/-}$ mice was significantly prolonged compared with that in *pFn*$^{+/+}$ littermates, and over half of the mice did not stop bleeding spontaneously (5 of 9) (Figure 1E). Likewise, recombinant hirudin also significantly prolonged the tail bleeding time in *pFn*$^{-/-}$ mice but not in *pFn*$^{+/+}$ mice (Figure 1E). We next examined whether transfusion of pFn could prevent excessive bleeding after high-dose anticoagulant treatment. WT mice were given a high dose of heparin (200 U, i.p.) and then treated with either i.v. PBS or pFn (1.5 mg/ml, 200 μl). After treatment with PBS, none of the mice (8 of 8) had stopped tail bleeding spontaneously at 20 minutes. However, the majority of the mice (5 of 8) treated with pFn achieved hemostasis (arrest of bleeding) within 20 minutes (17.27 minutes, 95% confidence interval [14.79 minutes, 19.75 minutes], $P < 0.05$) (Figure 1F). These findings suggest that pFn is important for hemostasis in individuals who are unable to generate fibrin normally, such as patients receiving anticoagulant therapy.

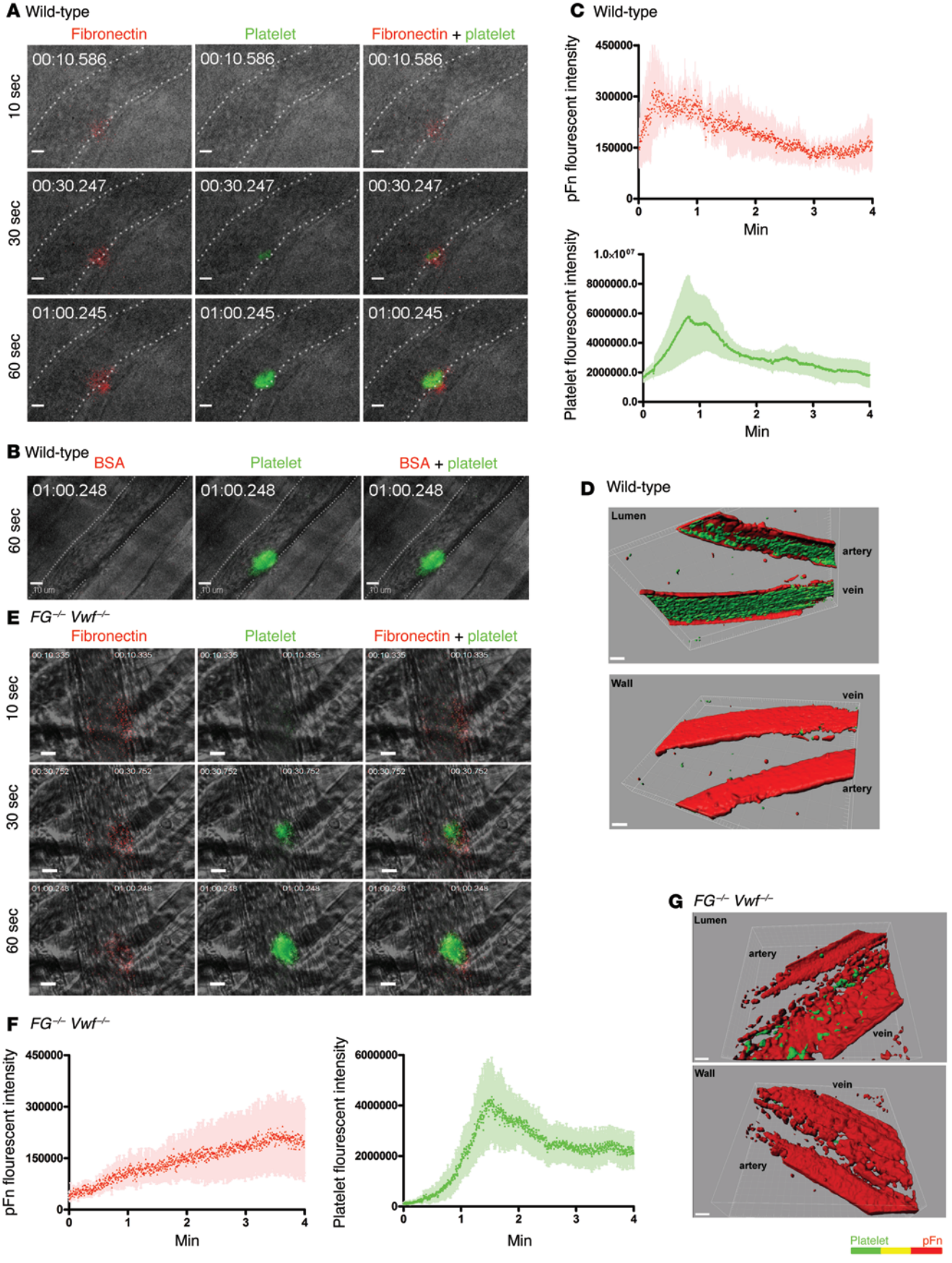
A Wild-type
Fibronectin
Platelet
Fibronectin + platelet
10 sec
30 sec
60 sec
00:10.586
00:30.247
01:00.245
B Wild-type
BSA
Platelet
BSA + platelet
01:00.248
C Wild-type
pFn flourescent intensity
Platelet flourescent intensity
Min
D Wild-type
Lumen
artery
vein
Wall
E FG-/- Vwf-/-
F FG-/- Vwf-/-
G FG-/- Vwf-/-
Platelet
pFn

Figure 2. pFn deposition is a hemostatic event preceding platelet accumulation. (**A**) pFn deposition and platelet accumulation in WT mice in the laser-induced cremaster arterial thrombosis model. pFn deposition at the injury site was apparent 10 seconds after laser injury, prior to significant platelet accumulation. (**B**) No deposition of fluorescently labeled BSA was observed. (**C**) pFn deposition and platelet accumulation at the site of injury of WT mice in the cremaster arterial thrombosis model were measured by fluorescence intensity. The curves represent pFn or platelet mean fluorescent intensity, and the shaded regions represent SEM (n = 5 in each group). (**D**) 3D reconstruction of pFn deposition and initial platelet accumulation in mesenteric arteries and veins 5 minutes after $FeCl_3$ injury in WT mice. The images shown are the longitudinal sections of the vessels, viewed from the inside of the lumen or from the outside the vessel wall. (**E**) pFn deposition and platelet accumulation in *FG*$^{-/-}$ *Vwf*$^{-/-}$ mice in the laser-induced cremaster arterial thrombosis model. (**F**) Measurement of fluorescent intensity of pFn deposition and platelet accumulation at the site of injury of *FG*$^{-/-}$ *Vwf*$^{-/-}$ mice in the cremaster arterial thrombosis model (n = 5 in each group). (**G**) 3D reconstruction of pFn deposition and initial platelet accumulation in mesenteric arteries and veins 5 minutes after $FeCl_3$ injury in *FG*$^{-/-}$ *Vwf*$^{-/-}$ mice. Scale bar: 10 μm (**A**, **B**, and **E**); 50 μm (**D** and **G**). All images shown are representative of at least 5 independent experiments.

pFn deposition is a hemostatic event preceding the classical first wave of hemostasis. It is widely accepted that platelet accumulation at the site of injury comprises the initial wave of hemostasis. Although we observed severe bleeding in the *FG*$^{-/-}$ *pFn*$^{-/-}$ mice, we previously and paradoxically found that depletion of pFn in *FG*$^{-/-}$ *Vwf*$^{-/-}$ mice enhances thrombus formation and stability (25). Thus, the life-threatening hemorrhage that we observed was likely not caused by a defect in platelet accumulation. To begin to explore the unique contributions of pFn to hemostasis, we examined the distribution of pFn at the site of vascular injury.

Using a laser injury cremaster arterial intravital microscopy model (25–27), we observed rapid deposition of fluorescently labeled pFn at sites of vessel injury in WT mice, whereas no BSA deposition was observed (Figure 2, A and B, and Supplemental Video 1). Interestingly, pFn deposited even prior to significant platelet accumulation (i.e., the classical first wave of hemostasis) (Figure 2A and Supplemental Video 1). Deposition of pFn was primarily found at the base of the growing hemostatic plug, which extended from the vessel wall into the bottom part of the hemostatic plugs adjacent to the vessel wall, colocalizing with approximately 45% (44.1% ± 3.4%) of the hemostatic plug (Figure 2A). pFn fluorescence intensity at the site of injury reduced as the platelet thrombi dissociated (Figure 2C). Importantly, pFn fluorescence in the thrombi gradually decreased as the thrombi extended into the vessel lumen, such that pFn was almost undetectable on the apical surface of the thrombi (Figure 2A). These findings suggest that in WT mice there is a gradient of pFn from the vessel wall (high pFn) to the apex of the thrombi (little or undetectable).

This process was further observed in WT mice under a laser scanning confocal microscope in a $FeCl_3$ injury mesenteric thrombosis model (18, 25). To exclude the possibility that the early detection of pFn in the previous cremaster arterial model was caused by greater microscope sensitivity for Alexa Fluor 488, we switched the labeling of pFn and platelets to Alexa Fluor 647 and DyLight 488, respectively. 3D reconstruction of the confocal images revealed that 5 minutes after $FeCl_3$ injury, the entire luminal side of the injured vessel wall (artery and vein) had been covered with a layer of deposited pFn (Figure 2D and Supplemental Video 2). In both veins and arteries, platelets accumulated on top of the pFn layer, indicating that pFn deposition occurred prior to platelet accumulation. This observation was consistent in all 5 mice studied: platelet fluorescence was only detectable on the luminal side, on top of the pFn layer already deposited.

We then studied whether pFn deposition persists in the absence of Fg and VWF using the laser injury cremaster arterial thrombosis model. As observed in the WT mice, the rapid deposition of fluorescently labeled pFn at sites of vessel injury in *FG*$^{-/-}$ *Vwf*$^{-/-}$ mice occurred prior to significant platelet accumulation (Figure 2E and Supplemental Video 1). Deposition of pFn was also primarily found at the base of the growing hemostatic plug. While platelet accumulation reached its maximum and began to dissociate at approximately 1.5 minutes, pFn continued to deposit and reached a plateau at approximately 3.5 minutes. The fluorescence intensity of pFn at the site of injury did not decrease as the platelets dissociated from the hemostatic plug (Figure 2F), and the amount of pFn deposition in *FG*$^{-/-}$ *Vwf*$^{-/-}$ mice was similar to that in WT mice during the 4-minute observation ($P > 0.05$, Supplemental Figure 4, A and B). These observations suggest that, in the absence of Fg and VWF, pFn can also deposit on the vessel wall prior to significant platelet accumulation but does not significantly incorporate into the growing platelet plug as compared with the WT mice.

Using confocal microscopy, marked pFn deposition was also observed in the $FeCl_3$ injury mesenteric thrombosis model in *FG*$^{-/-}$ *Vwf*$^{-/-}$ mice (Figure 2G and Supplemental Video 2). Platelets accumulated on top of the pFn layer, indicating that pFn deposition occurred prior to platelet accumulation. We confirmed that early pFn deposition occurred in injured cremaster and mesenteric vessels in *FG*$^{-/-}$ mice (Figure 3, A and B) and β3 integrin–deficient (*Itgβ3*$^{-/-}$) mice (Figure 3, C and D, and Supplemental Videos 1 and 2). Furthermore, after antibody-induced depletion of platelets in WT mice (28), similar deposition of pFn was observed on the injured vessel wall (Supplemental Figure 4C). pFn fluorescence was clearly visible at the site of injury 60 minutes after laser injury, even after the platelet thrombus dissociated from the vessel wall (Figure 3E), suggesting that pFn was incorporated into the subendothelial matrix.

After heparin treatment, minimal platelet accumulation was observed 5 minutes after injury, yet pFn deposition on the injured vessel wall remained similar to that in untreated WT controls (Figure 3F). Considering that most *pFn*$^{+/+}$ (but not *pFn*$^{-/-}$) mice treated with the same dose of heparin achieved hemostasis within 5 minutes in the tail bleeding assay (Figure 1E), these data suggest a major contribution of pFn in controlling bleeding following anticoagulant treatment.

Collagen is a major subendothelial matrix protein and can bind to the N terminus of pFn (8), but this process has not been well studied under flow conditions. Here, we found rapid deposition of pFn on collagen within 40 seconds when purified pFn was perfused over a collagen-coated surface under arterial shear rate, while no deposition of BSA was observed (Supplemental Figure 4D and Supplemental Video 3). This observation demonstrated that collagen could mediate the rapid and efficient deposition of pFn.

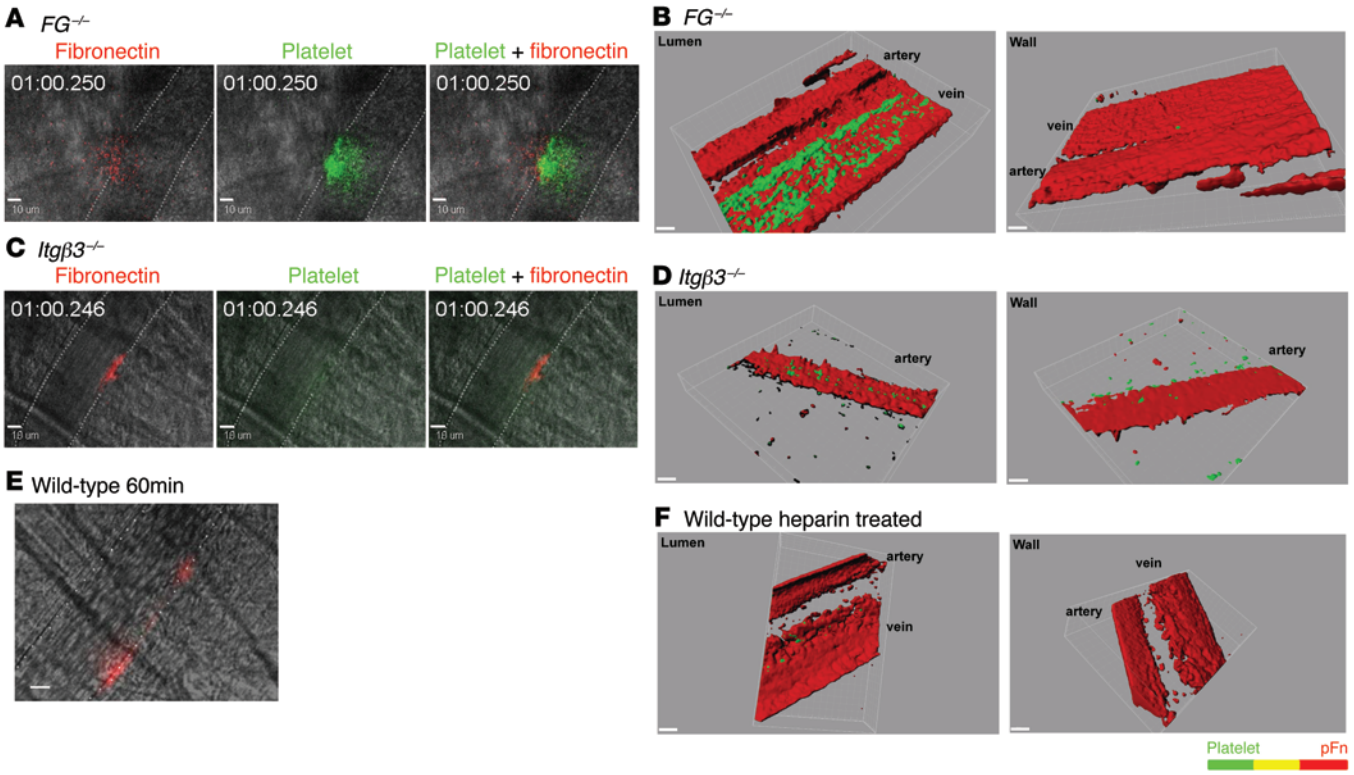

Figure 3. pFn deposition on the injured vessel wall is independent of Fg and β3 integrin and persists after heparin treatment. (**A**) pFn deposition and platelet accumulation in *FG*$^{-/-}$ mice in the laser-induced cremaster arterial thrombosis model. Images were taken at 1 minute after injury. (**B**) 3D reconstruction of pFn deposition and initial platelet accumulation in mesenteric arteries and veins 5 minutes after $FeCl_3$ injury in *FG*$^{-/-}$ mice. (**C**) pFn deposition and platelet accumulation in *Itgβ3*$^{-/-}$ mice in the laser-induced cremaster arterial thrombosis model. Images were taken at 1 minute after injury. (**D**) 3D reconstruction of pFn deposition and initial platelet accumulation in a mesenteric artery 5 minutes after $FeCl_3$ injury in a *Itgβ3*$^{-/-}$ mouse. (**E**) Fluorescently labeled pFn is detectable at the injury site 60 minutes after laser injury in WT mice. (**F**) 3D reconstruction of pFn deposition and initial platelet accumulation in mesenteric arteries and veins 5 minutes after $FeCl_3$ injury in WT mice treated with heparin. Scale bar: 10 μm (**A**, **C**, and **E**); 50 μm (**B**, **D**, and **F**). All images shown are representative of at least 5 independent experiments.

pFn reinforces the mechanical strength of fibrin clots. pFn can be covalently linked to fibrin by thrombin-activated FXIIIa and becomes incorporated into the fibrin clot (10). Using thromboelastography (TEG), fibrin clots formed in whole blood or platelet-poor plasma (PPP) from *pFn*$^{+/+}$ mice were significantly stronger than those formed in whole blood or PPP from *pFn*$^{-/-}$ littermates (Figure 4, A and B), although the rates of clot formation were similar in both groups (Supplemental Figure 5, A and B). The decrease in clot strength was not due to difference in Fg concentration (Supplemental Figure 6). Reintroduction of pFn into *pFn*$^{-/-}$ whole blood ameliorated the defect in clot strength (Figure 4C). Compared with adding PBS or BSA controls, the reintroduction of pFn to a final concentration of 300 μg/ml raised the maximum amplitude (MA) in *pFn*$^{-/-}$ blood to about 60% (Figure 4C). These findings suggest that pFn supports hemostasis not only through deposition at the injured vessel wall but also by enhancing the strength of the fibrin network.

pFn controls the diameter of fibrin fibers. We then studied the formation of the pFn-fibrin network in vitro. Fluorescently labeled murine pFn, which was purified from *FG*$^{-/-}$ mice, was actively recruited to the fibrin network formed in mouse PPP, resulting in thicker fibrin fibers compared with those in BSA-treated PPP (Figure 4D and Supplemental Figure 5C). Using scanning electron microscopy, we found that addition of 330 μg/ml pFn to *pFn*$^{-/-}$ mouse PPP significantly increased fibrin fiber diameter compared with addition of PBS alone (113.6 ± 2.8 nm and 69.4 ± 0.6 nm, respectively, $P < 0.01$) (Figure 4, E and F). Consistent with this, the diameter of fibrin fibers formed in PPP from *pFn*$^{+/+}$ mice was significantly larger than that formed in PPP from *pFn*$^{-/-}$ mice (Figure 4, H and I).

To examine whether pFn also controls the diameter of human fibrin fibers, a gelatin column was used to remove endogenous pFn from human PPP. Human pFn, BSA, or PBS were then added to the pFn-depleted PPP. We found that, as in the mouse PPP, pFn was actively recruited into the fibrin network (Figure 5A). After addition of 330 μg/ml human pFn, the diameter of fibrin fibers increased from 90.7 ± 2.8 nm to 147.2 ± 10.0 nm ($P < 0.01$, Figure 5, B and C). Consistent with the increased fiber diameter, fiber density decreased in the presence of pFn in both mouse and human plasma (Figure 4, G and J, and Figure 5D). These findings suggest that pFn modulates fibrin clot structure by enhancing the lateral aggregation of the fibrin protofibrils.

Non-fibrin-linked soluble pFn decreases platelet aggregation and thrombosis. The role of pFn in platelet aggregation remains controversial (29–32). Our earlier study showed that fibrin is required for the retention of pFn on the platelet surface (rendering pFn insoluble) (23). In the absence of Fg, platelet pFn content increases

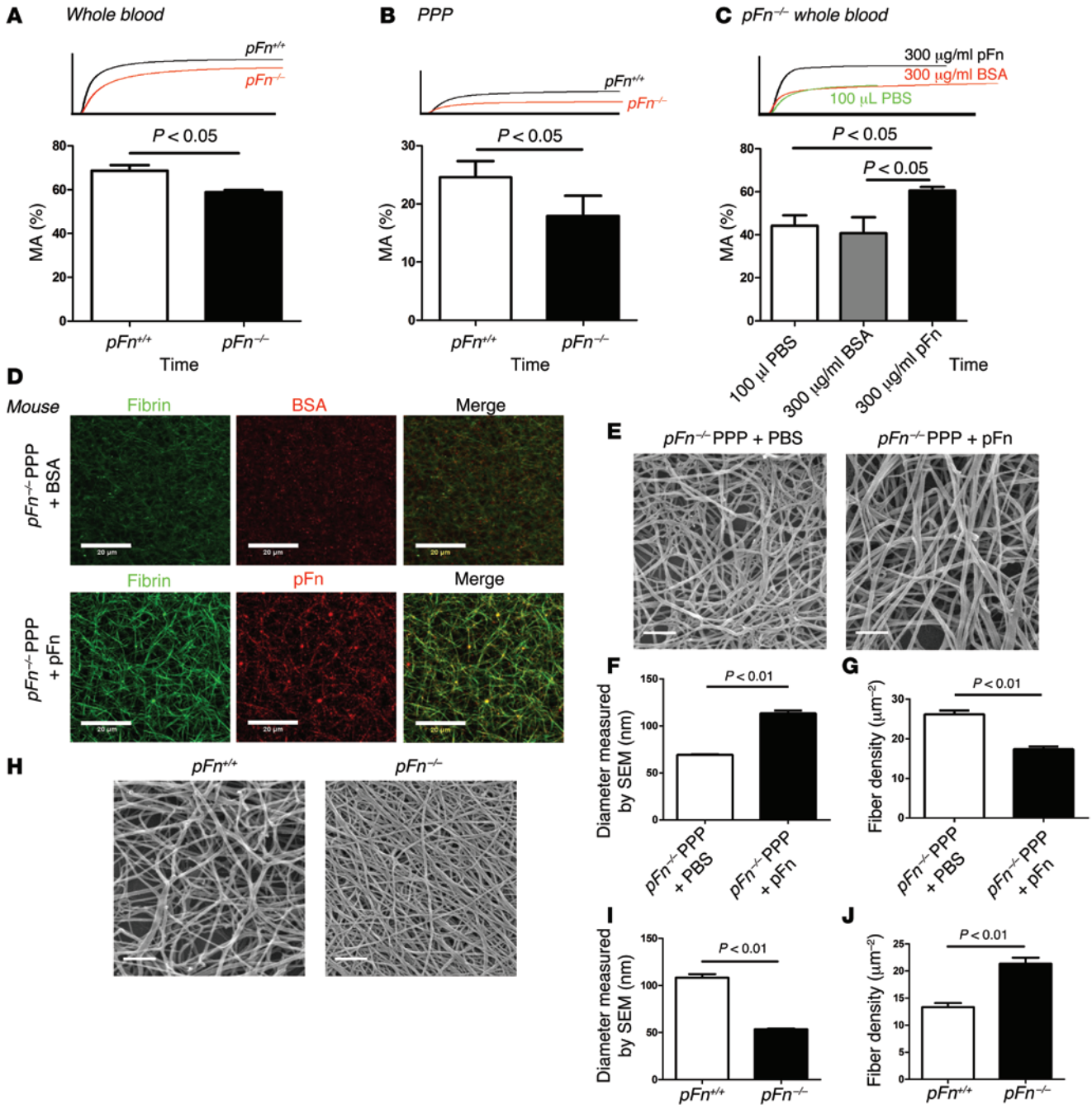

Figure 4. pFn enhances the mechanical strength of the fibrin clot and controls the diameter of fibrin fibers in mice. (**A**–**C**) Representative TEG tracings and MA measured by TEG in (**A**) whole blood and (**B**) PPP. (**C**) Adding back purified pFn partially rescued the MA of $pFn^{-/-}$ blood. n = 5 in each group. (**D**) Confocal images of mouse pFn-fibrin network formed in vitro (z projection of 11 individual slides taken at 1-μm interval across the 10-μm thickness of the clot). Mouse pFn or BSA was added into $pFn^{-/-}$ mouse PPP to a final concentration of 330 μg/ml. (**E**) Scanning electron microscopy analysis of mouse pFn-fibrin network formed in vitro. The same volume of PBS and mouse pFn was added into $pFn^{-/-}$ mouse PPP (final concentration 330 μg/ml). (**H**) Scanning electron microscopy analysis of $pFn^{+/+}$ and $pFn^{-/-}$ mouse pFn-fibrin network formed in vitro. pFn-fibrin network formation was initiated with 0.5 U/ml murine thrombin and 30 mM $CaCl_2$. (**F** and **I**) Average diameter of pFn-fibrin fibers formed in vitro. (**G** and **J**) Average density of pFn-fibrin fibers formed in vitro. Average diameter and density were calculated by counting the fibers crossed by 2 diagonal lines in a 1-μm^2 square. n = 9 in each group. Scale bar: 20 μm (**D**); 1 μm (**E** and **H**).

3- to 5-fold (17, 18). In our current study, we first found that in $FG^{-/-}$ mice this pool of pFn decreased aggregation of gel-filtered platelets (Figure 6A). In $Vwf^{-/-}$ mice, in which Fg was present, pFn enhanced aggregation of gel-filtered platelets induced by thrombin (which converts the platelet-released Fg to fibrin). However, when thrombin receptor-activating peptide (TRAP; AYPGKF, a potent PAR4-activating peptide) and collagen (neither of which convert Fg to fibrin) were used as an agonist in the same preparation of gel-filtered platelets, pFn attenuated platelet aggregation (Figure 6, B and C). ADP-induced platelet aggregation in $Vwf^{-/-}$

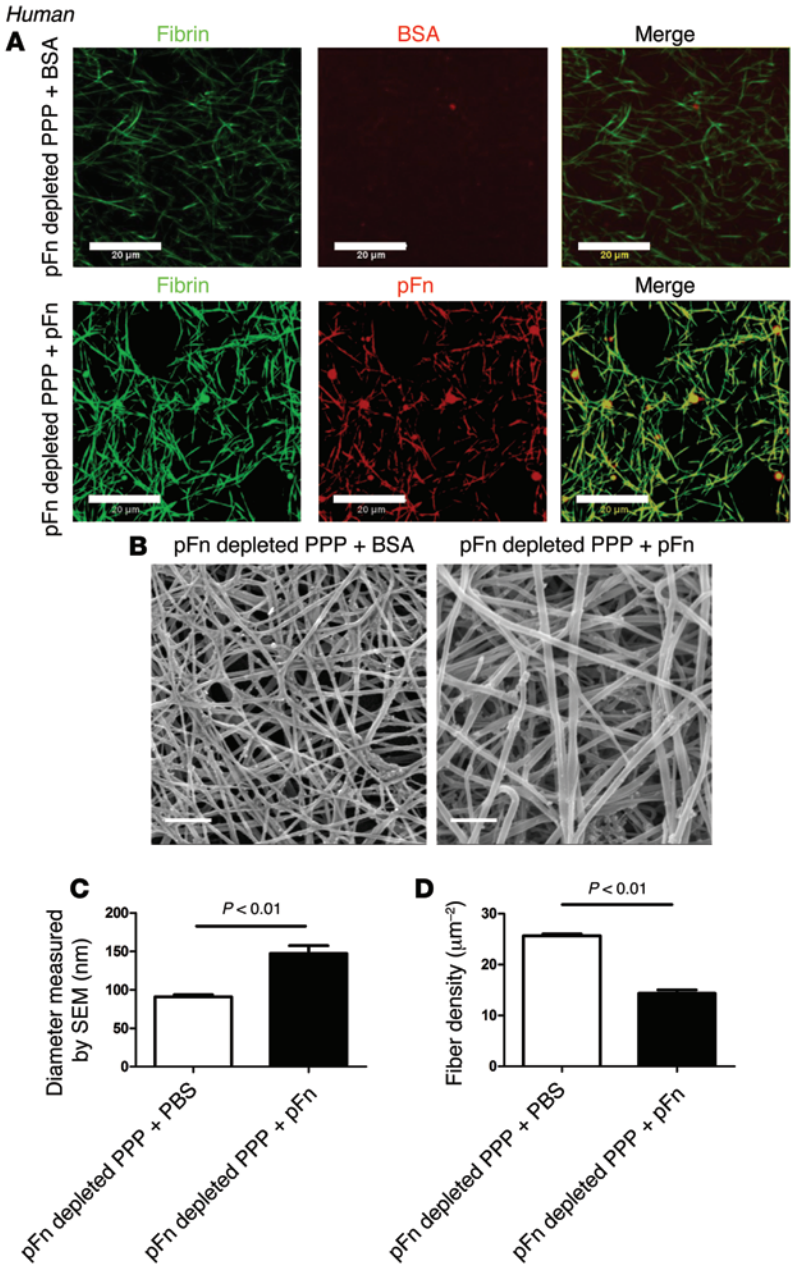

Figure 5. pFn controls the diameter of human fibrin fibers. (**A**) Confocal images of human pFn-fibrin network formed in vitro (z projection of 11 individual slides taken at 1-μm interval across the 10-μm thickness of the clot). Human pFn or BSA was added into pFn-depleted human PPP to a final concentration of 330 μg/ml. (**B**) Scanning electron microscopy analysis of human pFn-fibrin network formed in vitro. The same volume of PBS and human pFn was added into pFn-depleted human PPP (final concentration 330 μg/ml). (**C**) Average diameter of pFn-fibrin fibers formed in vitro. (**D**) Average density of pFn-fibrin fibers formed in vitro. Average diameter and density were calculated by counting the fibers crossed by 2 diagonal lines in a 1-μm^2 square. n = 10 in each group. Scale bar: 20 μm (**A**); 1 μm (**B**).

platelet-rich plasma (PRP) (which is unable to convert Fg to fibrin) was also enhanced after pFn depletion (Figure 6D). Therefore, in either $FG^{-/-}$ or $FG^{+/+}$ blood, as long as there is no fibrin generation, pFn plays a purely inhibitory role in platelet aggregation. Consistently, thrombin-induced gel-filtered platelet aggregation (in which platelet released Fg is converted to fibrin on platelet surface) was impaired in $pFn^{-/-}$ single-deficient mice as compared with that in $pFn^{+/+}$ littermate controls (Figure 6E). This demonstrated that the pFn contributes to platelet aggregation and suggested that fibrin plays a critical role in switching pFn from an inhibitory to a supportive role in platelet aggregation.

We next studied the role of pFn in thrombosis in $FG^{-/-}$ mice. Consistent with our previous observation in TKO mice (25), depletion of pFn in $FG^{-/-}$ mice enhanced thrombus formation in the ex vivo perfusion chamber model (Figure 6, F and G) and in vivo in the laser injury cremaster arterial thrombosis model (Figure 6, H and I). pFn therefore inhibits thrombus formation in mice lacking Fg (i.e., absence of Fg/fibrin).

Discussion

pFn was discovered as a protein that copurifies with Fg. It circulates in plasma in abundance and possesses the potential to assemble into fibrils that associate with various cell types, including platelets. Although it has long been suspected that pFn may play a role in the arrest of bleeding, its role in hemostasis has yet to be established. Here, we report an assessment of the role of pFn in hemostasis and thrombosis. We have demonstrated for the first time that, when fibrin formation is impaired, pFn is an essential survival factor; i.e., pFn is crucial for hemostasis in both $FG^{-/-}$ mice and in WT mice given anticoagulants. We found that pFn rapidly deposits onto the injured vessel wall, even prior to the classically recognized first wave of hemostasis, and remains at the site of injury. Through incorporation into the fibrin network, pFn controls the diameter of fibrin fibers and promotes the stability of the hemostatic plug. Interestingly, while pFn enhances platelet aggregation in the presence of fibrin, it inhibits platelet aggregation and thrombus formation in the absence of fibrin. This interaction with fibrin endows pFn with the capacity to switch from supporting hemostasis to inhibiting thrombosis/vessel occlusion, based on the fibrin gradient, in which fibrin decreases as it gets farther from the injured endothelium. These data establish pFn as an important hemostatic factor in Fg and coagulation deficiencies and a unique self-limiting regulator in thrombosis.

Current theory holds that platelet accumulation constitutes the first wave of hemostasis, and hemostatic events occurring before the platelet wave have not yet been adequately exposed. We have indicated that deposition of pFn at the site of injury is a key initial hemostatic process that occurs even earlier than the conventional first wave of hemostasis. These findings indicate the existence of a previously unrecognized "Fn" or "protein" wave of hemostasis before the classical platelet wave. While stable platelet plug formation usually requires sufficient time for platelets to adhere, activate, and aggregate, pFn and likely other plasma proteins accumulate on the subendothelial matrix immediately after injury. Importantly, the early deposited pFn can be noncova-

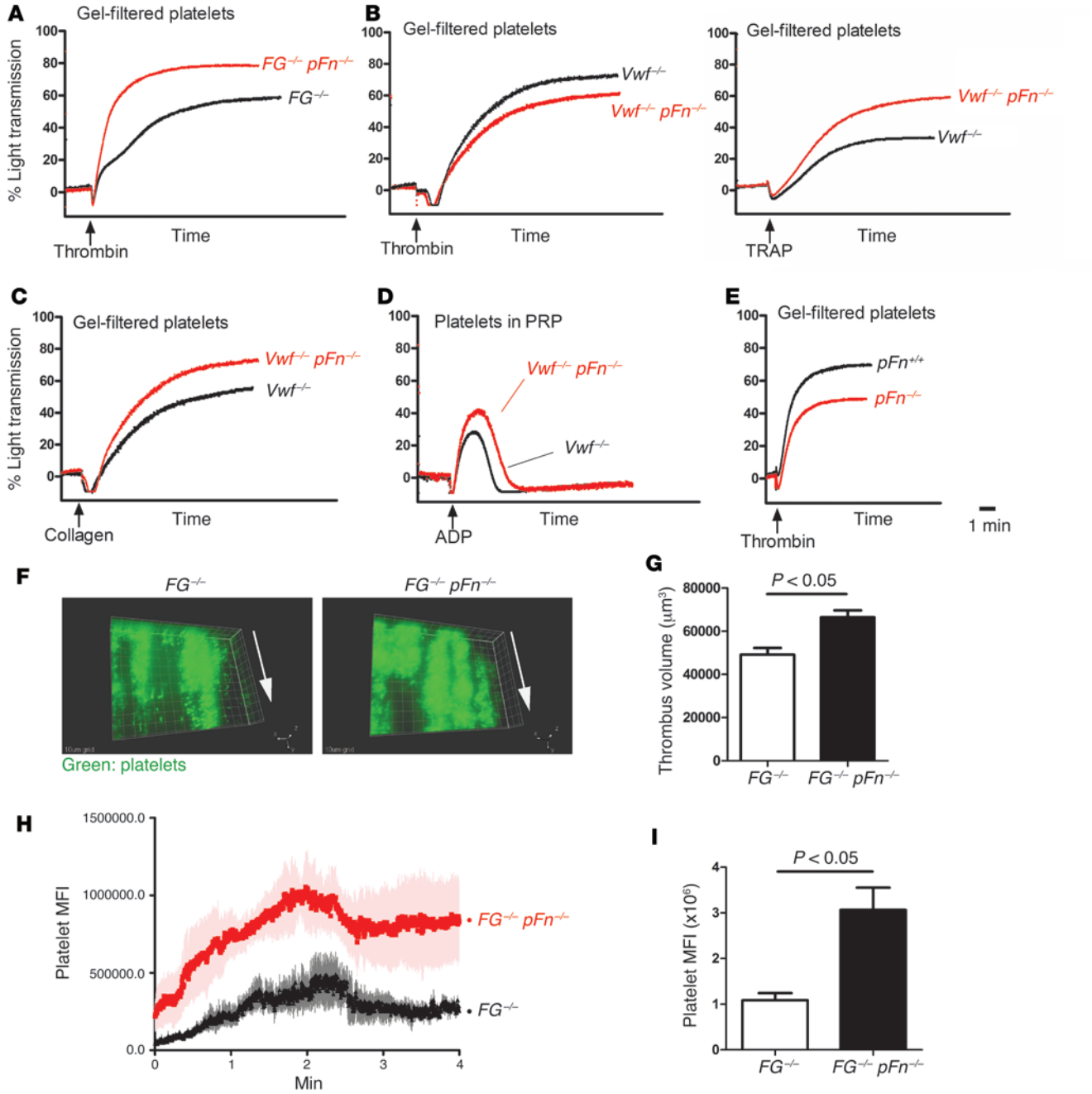

Figure 6. Role of pFn in platelet aggregation and thrombus formation in the presence or absence of fibrin. (**A**) Thrombin-induced (0.2 U/ml) *FG*$^{-/-}$ *pFn*$^{-/-}$ and *FG*$^{-/-}$ gel-filtered platelet aggregation. (**B**) Thrombin-induced (0.2 U/ml) or TRAP-induced (500 μM) *Vwf*$^{-/-}$ *pFn*$^{-/-}$ and *Vwf*$^{-/-}$ gel-filtered platelet aggregation. (**C**) Collagen-induced (20 μg/ml) *Vwf*$^{-/-}$ *pFn*$^{-/-}$ and *Vwf*$^{-/-}$ gel-filtered platelet aggregation. (**D**) ADP-induced (20 μM) *Vwf*$^{-/-}$ *pFn*$^{-/-}$ and *Vwf*$^{-/-}$ platelet aggregation in PRP. (**E**)Thrombin-induced (0.2 U/ml) *pFn*$^{+/+}$ and *pFn*$^{-/-}$ gel-filtered platelet aggregation. All representative tracings of platelet aggregation are shown from at least 3 independent experiments. (**F**) Thrombus formation in a collagen-coated perfusion chamber infused with blood from *FG*$^{-/-}$ *pFn*$^{-/-}$ mice and their *pFn*$^{+/+}$ *FG*$^{-/-}$ littermates (shear rate = 1,800 s^{-1}). Images were taken with a confocal microscopy after infusion for 3 minutes. Grid in the image represents 10 μm. (**G**) Thrombus volume measured 3 minutes after infusion. *n* = 5 in each group. (**H**) Thrombus formation in *FG*$^{-/-}$ *pFn*$^{-/-}$ mice and their *pFn*$^{+/+}$ *FG*$^{-/-}$ littermates observed in the laser-induced cremaster arterial thrombosis model. The curves represent pFn or platelet mean fluorescent intensity, and the shaded regions represent SEM. (**I**) The total area under the curve (AUC) was greater in *FG*$^{-/-}$ *pFn*$^{-/-}$ mice than in *FG*$^{-/-}$ mice. *n* = 5 in each group. Data are presented as mean ± SEM.

lently or covalently (via FXIIIa) linked to collagen (8), and the integrins on subendothelial cells and on the adhered platelets are able to assemble pFn into a matrix (14–16). Therefore, the deposition of pFn at the site of injury is likely a well-orchestrated matrix formation process that is crucial for the maintenance of vessel integrity. Together with FXIIIa and likely also protein disulfide isomerases (33), the initially deposited pFn may serve as a substrate to recruit other key proteins in hemostatic plug formation.

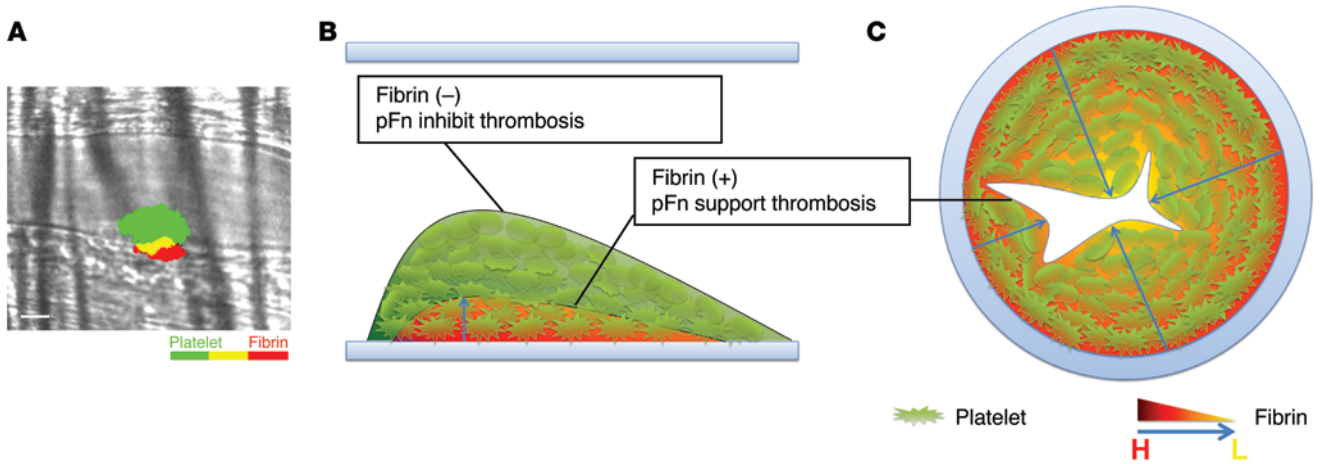

Figure 7. pFn is a self-limiting factor for hemostasis and thrombosis. (**A**) Platelet accumulation and fibrin formation in WT mice in the laser-induced cremaster arterial thrombosis model. Fibrin forms at the bottom of the platelet thrombi, while at the top of the growing thrombi, fibrin is nearly undetectable. Scale bar: 10 μm. (**B**) Illustration of the self-limiting role of pFn for thrombosis after vascular injury. pFn deposited at the base of the hemostatic plug likely cross-links with fibrin to support platelet aggregation. The soluble pFn at the top of the thrombi is associated with platelets but not with fibrin. These pFn molecules play a solely inhibitory role, stabilizing the thrombus and suppressing excessive thrombus buildup, thus helping to form a restricted local hemostatic plug that maintains hemostasis without causing downstream ischemia. (**C**) Illustration of pFn promoting efficient hemostasis after severe vascular injury. After severe trauma to a vessel, a large amount of thrombin is generated from multiple sites of the injured vessel wall, so that even at the top of the growing thrombi, there is a sufficient amount of thrombin to initiate fibrin formation. Under this condition, pFn is continuously incorporated onto the top of the growing thrombus through fibrin. This fibrin cross-linked pFn promotes the formation of an occlusive thrombus and helps to stop blood loss efficiently after severe vascular injuries. Blue arrows indicate fibrin concentration change from high level (H, red) to low level (L, yellow) as the hemostatic plug extends from the vessel wall into to the vessel lumen.

In addition to free pFn in the blood plasma, during hemostatic plug formation, platelets may serve as a transporter of pFn. Accumulating platelets carry and release their pFn content specifically at the injury site, which may markedly increase the local concentration of pFn. The released pFn may be directly organized on the activated platelet surface into a matrix to support hemostasis. This portion of platelet-transported pFn is likely to be more important for the maintenance of hemostasis in Fg deficiency, because we previously found that the pFn content in platelets increased 3- to 5-fold in both $FG^{-/-}$ mice and in patients with hypofibrinogenemia (18, 23, 24) as a result of increased uptake of pFn via the β3 integrin in the absence of Fg competition (17). The deposited pFn on the vessel wall may induce more platelet adhesion through a GPIb-pFn interaction (34), which could lead to more pFn release from the platelets. Therefore, the platelet-transported pFn further magnifies the initial "Fn" wave. Future investigation focusing on this "Fn" or "protein" wave of hemostasis will bring new insights into the initiation and maintenance of hemostasis.

In addition to local deposition and matrix formation at the site of injury, we demonstrated that pFn also contributes to hemostasis through its incorporation into clots. The effect of pFn on the mechanical characteristics of fibrin clots has been controversial. Addition of pFn to a reconstituted Fg solution resulted in increased clot shear modulus and turbidity (35, 36); however, other studies proposed that pFn may block fibrin polymerization, leading to prolonged clotting time, decreased turbidity (37), and reduced elasticity (38). This discrepancy is likely due to the methodology; all of these studies used reconstituted Fg solution rather than natural plasma, and the purity of reagents used was variable. The major challenge is to isolate pure pFn. pFn used in almost all of the previous studies was purified from healthy human subjects or WT mice and was therefore almost certainly contaminated with Fg or fibrin (Supplemental Figure 3B). Using pFn-deficient plasma and pFn purified from $FG^{-/-}$ mice, we were able to study, for the first time, the function of pFn in a natural plasma environment without Fg or fibrin contamination. We demonstrate that pFn increases the diameter of fibrin fibers and strengthens the fibrin clot, mainly by enhancing lateral aggregation and increasing fiber diameter. The mechanical and structural defects in $pFn^{-/-}$ fibrin clots are similar to those of a reported fibrin mutant deficient in lateral aggregation (39), suggesting that pFn enhances clot strength through enhancing lateral aggregation of fibrin protofibrils.

The role of pFn in platelet aggregation has been intensely debated for decades. While pFn has been shown to inhibit ionophore A23187- and collagen-induced platelet aggregation (29, 30), monoclonal antibodies against Fn inhibited platelet aggregation mediated by these agonists (31, 32). It has also been reported that pFn corrected a platelet aggregation defect in Ehlers-Danlos syndrome (a connective tissue disorder), although the mechanism is yet unclear (40). In our experiments, we found that thrombin-induced aggregation of gel-filtered platelets was significantly stronger in $pFn^{+/+}$ platelets than in $pFn^{-/-}$ platelets (Figure 6E), although it is difficult to distinguish the difference in platelet aggregation between platelets from $pFn^{-/-}$ mice and $pFn^{+/+}$ littermates induced either by ADP in PRP or TRAP and collagen in gel-filtered platelets. The inconsistency of the responses is likely due to different levels of fibrin generated during the sampling and in vitro experimental processes. Using our unique $FG^{-/-}$ $pFn^{-/-}$ mouse (absence of fibrin) and $Vwf^{-/-}$ $pFn^{-/-}$ mouse (minimal incidental fibrin generation due to low FVIII activity) strains, we minimized the incidental fibrin generation and demonstrated that the effect of pFn on platelet aggregation and thrombosis is dependent on the presence or absence of fibrin.

The 2 RGD motifs on the pFn dimer are in close proximity, rendering them unlikely to be easily accessed by integrins from 2 platelets. When the N terminus of pFn cross-links with fibrin, the large pFn-fibrin complex may then be able to bind to platelets at RGD motifs on pFn and/or fibrin. The multiple integrin-binding sites enable the pFn-fibrin complex to bridge integrins on 2 or more platelets to support platelet aggregation. However, in the absence of fibrin (e.g., afibrinogenemia, anticoagulant therapy) or at the top of the thrombi, where fibrin is undetectable (Figure 7A), pFn binds to platelet surface integrins and prevents their interaction with other more potent ligands, such as Fg and other prothrombotic ligands (18, 22, 25, 41, 42), and inhibits platelet aggregation.

The hemostatic process after a mild injury in vivo only leads to limited local activation of platelets and the coagulation system, without jeopardizing downstream blood supply (27, 43). Based on our results demonstrating the dual role of pFn, we propose a novel model to explain the fine balance between maintenance of hemostasis and prevention of vessel occlusion. Consistent with a previous in vivo study (26), we found that a large amount of fibrin is generated close to the injured vessel wall (Figure 7, A and B). Therefore, pFn deposited at the base of the hemostatic plug can be cross-linked with fibrin. Moreover, the collagen, pFn, and fibrin at the base of the thrombi further enhance the ability of activated platelets to assemble pFn (44–46). Conversely, the deposited pFn further supports extracellular matrix formation, fibrin network formation, and platelet aggregation. Unlike the abundance of fibrin adjacent to the injured vessel wall, as the thrombus extends into the vessel lumen, the generation of fibrin gradually decreases (Figure 7, A and B). In the absence of fibrin, the soluble pFn at the apical part of thrombi plays a solely inhibitory role, suppressing excessive thrombosis and downstream ischemia.

In contrast to a mild injury, when a severe trauma to the vessel occurs (e.g., severed vessels), a large amount of thrombin is generated from multiple sites of the injured vessel wall, so that even at the top of the growing thrombi, there is likely a sufficient amount of thrombin to initiate fibrin formation (Figure 7C). Continuous fibrin-pFn cross-linking at the top of the growing thrombi promotes the formation of an occlusive thrombus (or hemostatic plug) and helps to stop blood loss efficiently. Therefore, pFn appears to be a sensor for the degree of vascular injury and modulates the magnitude of the hemostatic response depending on the severity of injury.

Maintenance of such a pFn-mediated hemostatic balance may be crucial for the treatment of thrombotic and hemorrhagic diseases. First, the current anticoagulant and thrombolytic therapies are associated with a high incidence of life-threatening bleeding complications, which approaches 10% in patients receiving high-dose anticoagulants (47). Therefore, it will be important to study whether intravenous pFn transfusion could simultaneously maintain hemostasis and prevent vessel occlusion in patients with heart attack and stroke. Second, there is considerable variation of pFn concentration in the human population (20). Notably, congenital low pFn (about 50% of normal pFn level) has been reported in a family (48). Although these variations in pFn level do not cause an overt bleeding phenotype under normal conditions, it may be of importance to study whether low pFn level is associated with excessive hemorrhage after trauma and surgery. It will also be important to investigate the relationship of pFn level (e.g., low pFn level in patients with acute liver failure or severe cirrhosis) with bleeding complications associated with anticoagulant therapy. Furthermore, given that pFn is a major intrinsic component of many blood products, the role of pFn in blood transfusion, especially its potential hemostatic and antithrombotic benefit in transfusion recipients, requires further study.

In summary, we have identified a new "Fn" or "protein" wave that occurs even earlier than the well-accepted first wave of hemostasis (i.e., platelet accumulation). We have also placed pFn as a component in the final steps of the coagulation cascade as a key factor that controls lateral aggregation of fibrin fibers. Moreover, we provided an explanation as to why the roles of pFn were previously controversial by demonstrating that it indeed has opposite effects (i.e., inhibitive and supportive) on platelet aggregation and identified that fibrin dictates the pFn functional switch. Further clinical investigation may lead to the development of pFn transfusion as a unique therapeutic strategy to control bleeding and modulate thrombosis.

Methods

Further details are available in the Supplemental Methods.

Materials. DyLight 649 and DyLight 488 fluorescent labeled anti-GPIb antibodies and JON/A (antibody against mouse-activated GPIIbIIIa) were purchased from Emfret Analytics. Alexa Fluor 488 and Alexa Fluor 647 protein labeling kits were purchased from Life Technologies Inc. Human Fg was purchased from Sigma-Aldrich. Recombinant hirudin was provided by Jawed Fareed at Loyola University, Chicago, Illinois, USA.

Mice. $pFn^{-/-}$ conditional knockout mice ($Fn^{fl/fl}$ Cre^{+}) and control littermates ($Fn^{fl/fl}$ Cre^{-}) were originally generated in the laboratory of Reinhard Fässler (Max Planck Institute of Biochemistry, Martinsried, Germany) (21). $Vwf^{-/-}$ $pFn^{-/-}$ and $FG^{-/-}$ $pFn^{-/-}$ mice were generated by breeding female pFn conditional knockout ($Fn^{fl/fl}$ Cre^{+}) mice with male $Vwf^{-/-}$ mice or male $FG^{-/-}$ mice, respectively. Genotype was detected by polymerase chain reaction and confirmed by Western blot. pFn depletion was induced by 3 i.p. injections of 250 μg polyinonic-polycytidylic acid (Sigma-Aldrich) into Cre^{+} and Cre^{-} littermates at 2-day intervals. pFn depletion in the plasma and platelets was confirmed by Western blot.

Bleeding time. The bleeding time assay was modified from the procedure previously described (49). After anesthetizing 6- to 8-week-old mice with 2.5% tribromoethanol (0.015 ml/g) and maintaining them at 37°C with a heating pad, the tip of the tail (2 mm) was amputated with a sharp scalpel. In most $Vwf^{-/-}$ and $Vwf^{-/-}$ $pFn^{-/-}$ mice, tail bleeding did not stop within 20 minutes of severing the tail tip. Therefore, instead of cutting the tail, one of the tail veins was punctured 4 cm from the tip of the tail. The injured tail was immediately placed into warm PBS maintained at 37°C, and the bleeding time was recorded from the time of injury until 10 seconds after bleeding had ceased. Bleeding time assay was terminated at 20 minutes, and mice that bled beyond this end point were counted as 20 minutes. For mice transfused with 200 μl PBS, pFn, or BSA, we extended the end point of the tail bleeding assay to 30 minutes.

Preparation of plasma, platelets, and pFn. Mouse plasma and platelets were prepared as previously described (18, 22, 25, 50–52). For pFn-fibrin clot formation in vitro, blood was drawn from inferior vena cava with a 25-gauge needle and immediately mixed with 3.2%

sodium citrate (1:9, vol/vol). pFn was isolated from $FG^{-/-}$ mice using gelatin-sepharose chromatography. The purity of pFn was evaluated by SDS-PAGE analysis. The presence of contaminating Fg was detected by Western blotting using a rabbit anti-human Fg antibody that also detected mouse Fg (American Diagnostica).

Intravital microscopy. The laser-induced cremaster arterial thrombosis model was performed as previously described (25, 26, 53, 54). Alexa Fluor 488–labeled pFn (5 μg) and DyLight 649 anti-GPIb antibodies (1 μg per 1 g body weight) were injected through the jugular vein cannula prior to injury. For detection of fibrin formation, an Alexa Fluor 488–labeled mouse anti-human fibrin IIβ chain antibody (2 μg per g body weight, Accurate Chemical) was injected prior to laser injury. Multiple independent injuries were induced on cremaster arterioles using an Olympus BX51W1 microscope equipped with a pulsed nitrogen dye laser. The dynamic deposition of pFn onto the injured vessel wall and the formation of the hemostatic plug were captured and analyzed using Slidebook software (Intelligent Imaging Innovations).

Confocal microscopy. $FeCl_3$-induced mesenteric arterial thrombosis was produced as previously described (18, 55, 56). After initiation of $FeCl_3$ injury, pFn deposition and thrombus formation were recorded using a Zeiss LSM 700 confocal laser scanning microscope (Zeiss). pFn (5 μg, i.v.) was labeled with Alexa Fluor 647 fluorescent dye, and platelets were labeled with Dylight 488 anti-GPIb antibodies (1 μg per 1 g body weight). The confocal data were analyzed using ZEN 2010 software (Zeiss), and 3D reconstruction of the images was produced by Imaris x64 (Bitplane). The same microscopy and software settings were applied in all experiments.

TEG. Blood obtained from the inferior vena cava of mice using a 25-gauge needle was immediately mixed with 3.2% sodium citrate at a 9:1 ratio. Whole blood and PPP were tested in a TEG 5000 Analyzer (Hemoscope).

pFn-fibrin network formation in vitro. pFn-fibrin network formation in vitro was evaluated as previously described (57). For experiments with human plasma, human PPP was added to the gelatin column. The column pass-through contained minimal amounts of pFn, as determined by Western blot analysis. pFn-depleted human PPP was used to assess human pFn-fibrin network formation in vitro.

Statistics. Data are presented as mean ± SEM. Statistical significance was assessed by the Student's unpaired (2-tailed) t test or the χ^2 test with Yates' correction. $P < 0.05$ was considered statistically significant. For statistical analysis of anticoagulant-treated mice (all of which could not stop bleeding), 95% confidence interval of bleeding time in the control group (which could stop bleeding) was calculated for the determination of statistical significance.

Study approval. All animal studies were approved by the Animal Care Committee of St. Michael's Hospital. All experimental procedures using human plasma were approved by the Research Ethics Board of St. Michael's Hospital. Human blood samples were drawn from antecubital veins of healthy volunteers after they provided informed consent according to guidelines provided by the Research Ethics Board of St. Michael's Hospital.

Acknowledgments

We thank Reinhard Fässler for providing the pFn conditional knockout mice and for his valuable suggestions and comments during manuscript preparation. We thank Jay L. Degen and Denisa D. Wagner for providing the *FG*- and *Vwf*-deficient mice, respectively. We thank Henry Hong and Audrey Darabie for their assistance with scanning electron microscopy. We thank Pingguo Chen, Xi Lei, Xun Fu, and Emily C. Reddy for their assistance and valuable comments during the manuscript preparation. This work was supported by the Canadian Institutes of Health Research (CIHR, MOP 119540), Heart and Stroke Foundation of Canada (Ontario), and the CIHR team grant in venous thromboembolism. Equipment funds were from the Canada Foundation for Innovation, Canadian Blood Services, and St. Michael's Hospital. Y. Wang is a recipient of a PhD graduate fellowship from Canadian Blood Services and a Meredith and Malcolm Silver Scholarship in Cardiovascular Studies.

Address correspondence to: Heyu Ni, Department of Laboratory Medicine and Pathobiology, Department of Physiology, and Department of Medicine, University of Toronto and, Canadian Blood Services, St. Michael's Hospital, Room 420, LKSKI – Keenan Research Centre for Biomedical Science, 209 Victoria Street, Toronto, Ontario, Canada, M5B 1W8. Phone: 416.847.1738; E-mail: nih@smh.ca.

Some of the data from this manuscript have been orally presented at the Hot topics' talk at the 2012 Gordon Research Conference: Hemostasis, Waterville Valley, New Hampshire, USA, July 22–27, 2012; XXIV congress of the ISTH, Amsterdam, Netherlands, June 29–July 4, 2013; and the 52nd annual meeting of the American Society of Hematology, Orlando, Florida, USA, December 4–7, 2010.

1. Hynes RO. Hemostasis and thrombosis. In: Hynes RO, ed. *Fibronectins*. New York, New York, USA: Springer New York; 1990:335–348.
2. Savage B, Almus-Jacobs F, Ruggeri ZM. Specific synergy of multiple substrate-receptor interactions in platelet thrombus formation under flow. *Cell*. 1998;94(5):657–666.
3. Ni H, Freedman J. Platelets in hemostasis and thrombosis: role of integrins and their ligands. *Transfus Apher Sci*. 2003;28(3):257–264.
4. Ruggeri ZM. Platelets in atherothrombosis. *Nat Med*. 2002;8(11):1227–1234.
5. George EL, Georges-Labouesse EN, Patel-King RS, Rayburn H, Hynes RO. Defects in mesoderm, neural tube and vascular development in mouse embryos lacking fibronectin. *Development*. 1993;119(4):1079–1091.
6. Zerlauth G, Wolf G. Plasma fibronectin as a marker for cancer and other diseases. *Am J Med*. 1984;77(4):685–689.
7. Tomasini-Johansson B, Mosher DF. Plasma fibronectin concentration in inbred mouse strains. *Thromb Haemost*. 2009;102(6):1278–1280.
8. Mosher DF, Schad PE. Cross-linking of fibronectin to collagen by blood coagulation Factor XIIIa. *J Clin Invest*. 1979;64(3):781–787.
9. Moretti FA, Chauhan AK, Iaconcig A, Porro F, Baralle FE, Muro AF. A major fraction of fibronectin present in the extracellular matrix of tissues is plasma-derived. *J Biol Chem*. 2007;282(38):28057–28062.
10. Mosher DF. Cross-linking of cold-insoluble globulin by fibrin-stabilizing factor. *J Biol Chem*. 1975;250(16):6614–6621.
11. Doolittle RF. Step-by-step evolution of vertebrate blood coagulation. *Cold Spring Harb Symp Quant Biol*. 2009;74:35–40.
12. Tucker RP, Chiquet-Ehrismann R. Evidence for the evolution of tenascin and fibronectin early in the chordate lineage. *Int J Biochem Cell Biol*. 2009;41(2):424–434.
13. Ghosh A, et al. Characterization of zebrafish von Willebrand factor reveals conservation of domain structure, multimerization, and intracellular storage. *Adv Hematol*. 2012;2012:214209.
14. McKeown-Longo PJ, Mosher DF. Binding of plasma fibronectin to cell layers of human skin fibroblasts. *J Cell Biol*. 1983;97(2):466–472.

15. Olorundare OE, Peyruchaud O, Albrecht RM, Mosher DF. Assembly of a fibronectin matrix by adherent platelets stimulated by lysophosphatidic acid and other agonists. *Blood*. 2001;98(1):117–124.
16. Cho J, Mosher DF. Characterization of fibronectin assembly by platelets adherent to adsorbed laminin-111. *J Thromb Haemost*. 2006;4(5):943–951.
17. Ni H, Papalia JM, Degen JL, Wagner DD. Control of thrombus embolization and fibronectin internalization by integrin alpha IIb beta 3 engagement of the fibrinogen gamma chain. *Blood*. 2003;102(10):3609–3614.
18. Ni H, et al. Persistence of platelet thrombus formation in arterioles of mice lacking both von Willebrand factor and fibrinogen. *J Clin Invest*. 2000;106(3):385–392.
19. Ni H, et al. Plasma fibronectin promotes thrombus growth and stability in injured arterioles. *Proc Natl Acad Sci U S A*. 2003;100(5):2415–2419.
20. Cho J, Mosher DF. Role of fibronectin assembly in platelet thrombus formation. *J Thromb Haemost*. 2006;4(7):1461–1469.
21. Sakai T, et al. Plasma fibronectin supports neuronal survival and reduces brain injury following transient focal cerebral ischemia but is not essential for skin-wound healing and hemostasis. *Nat Med*. 2001;7(3):324–330.
22. Yang H, et al. Fibrinogen and von Willebrand factor-independent platelet aggregation in vitro and in vivo. *J Thromb Haemost*. 2006;4(10):2230–2237.
23. Zhai Z, et al. Fibrinogen controls human platelet fibronectin internalization and cell-surface retention. *J Thromb Haemost*. 2007;5(8):1740–1746.
24. Xu X, et al. A novel fibrinogen Bbeta chain frameshift mutation in a patient with severe congenital hypofibrinogenaemia. *Thromb Haemost*. 2006;95(6):931–935.
25. Reheman A, et al. Plasma fibronectin depletion enhances platelet aggregation and thrombus formation in mice lacking fibrinogen and von Willebrand factor. *Blood*. 2009;113(8):1809–1817.
26. Falati S, Gross P, Merrill-Skoloff G, Furie BC, Furie B. Real-time in vivo imaging of platelets, tissue factor and fibrin during arterial thrombus formation in the mouse. *Nat Med*. 2002;8(10):1175–1181.
27. Stalker TJ, et al. Hierarchical organization in the hemostatic response and its relationship to the platelet-signaling network. *Blood*. 2013;121(10):1875–1885.
28. Webster ML, et al. Relative efficacy of intravenous immunoglobulin G in ameliorating thrombocytopenia induced by antiplatelet GPIIbIIIa versus GPIbalpha antibodies. *Blood*. 2006;108(3):943–946.
29. Moon DG, Kaplan JE, Mazurkewicz JE. The inhibitory effect of plasma fibronectin on collagen-induced platelet aggregation. *Blood*. 1986;67(2):450–457.
30. Santoro SA. Inhibition of platelet aggregation by fibronectin. *Biochem Biophys Res Commun*. 1983;116(1):135–140.
31. Dixit VM, et al. Inhibition of platelet aggregation by a monoclonal antibody against human fibronectin. *Proc Natl Acad Sci U S A*. 1985;82(11):3844–3848.
32. Thurlow PJ, Kenneally DA, Connellan JM. The role of fibronectin in platelet aggregation. *Br J Haematol*. 1990;75(4):549–556.
33. Furie B, Flaumenhaft R. Thiol isomerases in thrombus formation. *Circ Res*. 2014;114(7):1162–1173.
34. Beumer S, Heijnen HF, IJsseldijk MJ, Orlando E, de Groot PG, Sixma JJ. Platelet adhesion to fibronectin in flow: the importance of von Willebrand factor and glycoprotein Ib. *Blood*. 1995;86(9):3452–3460.
35. Kamykowski GW, Mosher DF, Lorand L, Ferry JD. Modification of shear modulus and creep compliance of fibrin clots by fibronectin. *Biophys Chem*. 1981;13(1):25–28.
36. Okada M, Blomback B, Chang MD, Horowitz B. Fibronectin and fibrin gel structure. *J Biol Chem*. 1985;260(3):1811–1820.
37. Niewiarowska J, Cierniewski CS. Inhibitory effect of fibronectin on the fibrin formation. *Thromb Res*. 1982;27(5):611–618.
38. Procyk R, King RG. The elastic modulus of fibrin clots and fibrinogen gels: the effect of fibronectin and dithiothreitol. *Biopolymers*. 1990;29(3):559–565.
39. Collet JP, et al. The alphaC domains of fibrinogen affect the structure of the fibrin clot, its physical properties, and its susceptibility to fibrinolysis. *Blood*. 2005;106(12):3824–3830.
40. Arneson MA, Hammerschmidt DE, Furcht LT, King RA. A new form of Ehlers-Danlos syndrome. Fibronectin corrects defective platelet function. *JAMA*. 1980;244(2):144–147.
41. Dunne E, et al. Cadherin 6 has a functional role in platelet aggregation and thrombus formation. *Arterioscler Thromb Vasc Biol*. 2012;32(7):1724–1731.
42. Wang Y, et al. Platelets in thrombosis and hemostasis: old topic with new mechanisms. *Cardiovasc Hematol Disord Drug Targets*. 2012;12(2):126–132.
43. Brass LF, Wannemacher KM, Ma P, Stalker TJ. Regulating thrombus growth and stability to achieve an optimal response to injury. *J Thromb Haemost*. 2011;9(suppl 1):66–75.
44. Cho J, Mosher DF. Impact of fibronectin assembly on platelet thrombus formation in response to type I collagen and von Willebrand factor. *Blood*. 2006;108(7):2229–2236.
45. Cho J, Mosher DF. Enhancement of thrombogenesis by plasma fibronectin cross-linked to fibrin and assembled in platelet thrombi. *Blood*. 2006;107(9):3555–3563.
46. Cho J, Degen JL, Coller BS, Mosher DF. Fibrin but not adsorbed fibrinogen supports fibronectin assembly by spread platelets. Effects of the interaction of alphaIIb beta3 with the C terminus of the fibrinogen gamma-chain. *J Biol Chem*. 2005;280(42):35490–35498.
47. Melloni C, et al. Gibler WB, Ohman EM, and Peterson ED. Unfractionated heparin dosing and risk of major bleeding in non-ST-segment elevation acute coronary syndromes. *Am Heart J*. 2008;156(2):209–215.
48. Shirakami A, et al. Plasma fibronectin deficiency in eight members of one family. *Lancet*. 1986;1(8479):473–474.
49. Chen J, et al. N-acetylcysteine reduces the size and activity of von Willebrand factor in human plasma and mice. *J Clin Invest*. 2011;121(2):593–603.
50. Yang H, et al. Fibrinogen is required for maintenance of platelet intracellular and cell-surface P-selectin expression. *Blood*. 2009; 114(2):425–436.
51. Li C, et al. The maternal immune response to fetal platelet GPIbalpha causes frequent miscarriage in mice that can be prevented by intravenous IgG and anti-FcRn therapies. *J Clin Invest*. 2011;121(11):4537–4547.
52. Ni H, Ramakrishnan V, Ruggeri ZM, Papalia JM, Phillips DR, Wagner DD. Increased thrombogenesis and embolus formation in mice lacking glycoprotein V. *Blood*. 2001;98(2):368–373.
53. Lei X, et al. Anfibatide, a novel GPIb complex antagonist, inhibits platelet adhesion and thrombus formation in vitro and in vivo in murine models of thrombosis. *Thromb Haemost*. 2014;111(2):279–289.
54. Sachs UJ, Nieswandt B. In vivo thrombus formation in murine models. *Circ Res*. 2007;100(7):979–991.
55. Yang Y, et al. Plant food delphinidin-3-glucoside significantly inhibits platelet activation and thrombosis: novel protective roles against cardiovascular diseases. *PloS One*. 2012;7(5):e37323.
56. Reheman A, et al. Vitronectin stabilizes thrombi and vessel occlusion but plays a dual role in platelet aggregation. *J Thromb Haemost*. 2005;3(5):875–883.
57. Campbell RA, Overmyer KA, Selzman CH, Sheridan BC, Wolberg AS. Contributions of extravascular and intravascular cells to fibrin network formation, structure, and stability. *Blood*. 2009;114(23):4886–4896.